

Prominent field for shape processing of archaeological artifacts

Michael Kolomenkin
Technion

michkol@tx.technion.ac.il

Ilan Shimshoni
University of Haifa

ishimshoni@mis.haifa.ac.il

Ayellet Tal
Technion

ayellet@ee.technion.ac.il

Abstract

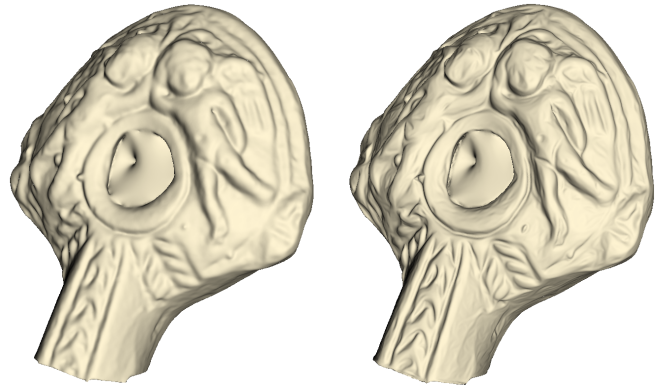
Archaeological artifacts are of vital importance in archaeological research. We propose a new approach for automatic processing of scanned artifacts. It is based on the definition of a new direction field on surfaces (a normalized vector field), termed the prominent field. We demonstrate the applicability of the prominent field in two applications. The first is surface enhancement of archaeological artifacts, which helps enhance eroded features and remove scanning noise. The second is artificial coloring that can replace manual artifact illustration in archaeological reports.

1. Introduction

Man-made artifacts are a major source of our knowledge about the past. Archaeologists who study assemblages of artifacts seek to identify distinctive patterns in them, which can be used for analysis and comparison. In order to disseminate the information about artifacts, these are either illustrated in reports or scanned by 3D scanners. Nowadays, 3D representations are becoming more popular, since they provide more information by allowing the archaeologist to view the artifact from different viewpoints at various scales and perform comparative measurements. Therefore, this paper focuses on 3D representation of artifacts. Specifically, we concentrate on artifacts with reliefs, which consist of a detailed surface, the *relief*, which resides on top of a smooth surface.

The main task facing the archaeologists is the analysis of these artifacts. This is done in several ways – accurately illustrating them by highlighting the surface edges, comparing artifact styles, classifying them etc. All these tasks can be facilitated by applying computer vision and computer graphics techniques [3, 11, 14, 21]. However, the 3D representation is often flawed, either due to noise added in the scanning process or due to defects in the original artifacts, such as erosion.

This paper addresses this problem by proposing a novel framework for processing the artifacts. It is based on a definition of a new direction field (a normalized vector field),



(a) Bilateral filtering [8]

(b) Our filtering

Figure 1. Enhancement of a late Hellenistic oil lamp from the first century BCE

termed the *prominent field*, defined for every point on the surface. This field is constructed to be smooth on the surface. Intuitively, the direction of this prominent field, termed the *prominent direction*, is perpendicular to the surface features. In this paper we consider the surface edges as its features.

Since this prominent field is closely related to the features of the relief surface, it is beneficial for a variety of processing applications. We demonstrate its effectiveness in two applications: adaptive filtering and artificial coloring. The goal of adaptive filtering is to enhance the features while keeping the surface intact. This may also help to remove the scanning noise. We propose to smooth the surface using the prominent field along the features and enhance it in the prominent direction (Figure 1). As a second application, we present a method for artificially coloring objects. The key idea is to color the surface according to its normal curvature in the prominent direction. This coloring increases the color contrast on the features, thus enhancing them.

The contribution of this paper is hence threefold:

- We define the prominent field and show how to compute it in interactive time (Section 2).

- We demonstrate how to employ the prominent field for surface smoothing and enhancement (Section 3).
- We propose a new method for artificial surface coloring that emphasizes the object features (Section 4).

2. Prominent field

This section presents a novel direction field – the *prominent field*. The prominent field should satisfy two requirements. First, it should be perpendicular to the surface edges. Second, it should be smooth on the whole surface, including the featureless regions. A field satisfying these requirements can enable us for example to enhance features in the direction of the field, while removing noise in the perpendicular direction.

Below, we first present the background required for the definition of the prominent field, the assumed surface model, and the surface curves. Next we define the prominent directions on the features. Finally, we define the smooth prominent field on the whole surface and present an algorithm that computes it.

2.1. Surface model

We assume that we are given a relief surface, which consists of a smooth, low frequency *base* and a high frequency *image* [12]. The image is represented as a function defined on the base, i.e., every point on the base corresponds to a single point on the image. In practice, this surface is given as a triangular mesh.

Formally, given a surface $S(u, v) : \mathbb{R}^2 \rightarrow \mathbb{R}^3$, we assume that it consists of a smooth base $B(u, v) : \mathbb{R}^2 \rightarrow \mathbb{R}^3$ and a function (image) $I(u, v) : \mathbb{R}^2 \rightarrow \mathbb{R}$ defined on B :

$$S(u, v) = B(u, v) + \bar{\mathbf{n}}(u, v)I(u, v), \quad (1)$$

where u and v are the coordinates of a parameterization and $\bar{\mathbf{n}}(u, v) : \mathbb{R}^2 \rightarrow \mathbb{S}^2$ is the normal of B (\mathbb{S}^2 being the unit sphere). We assume that B is locally a manifold and that its curvature has a smaller value than the curvature of I . Note that the image I can obtain both positive and negative values. (see Figure 2)

A relief surface can be viewed as a terrain having ridges, valleys, and relief edges, as illustrated in Figure 3. Ridges (valleys) are defined as the maximum (minimum) of the normal curvature in the first principal direction [6]. Relief edges run on the slopes between ridges and valleys and are parallel to them. They are shown to correspond to the image edges of the local image I [12]. Equivalently, they are defined as zero crossings of the curvature in the direction of the step edge model that best approximates the surface locally in the L_2 norm.

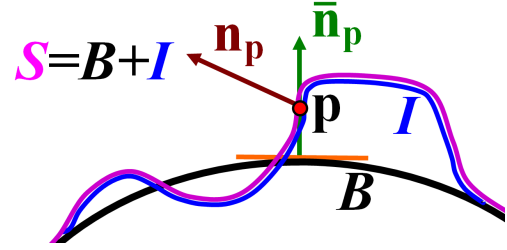


Figure 2. The surface S (magenta) is composed of a smooth base B (black) and a function I (blue). Function I at point \mathbf{p} can be locally viewed as an image defined on the tangent plane (orange) of the base. Point \mathbf{p} is a relief edge point if it is an edge point of this image. The normal $\mathbf{n}_{\mathbf{p}}$ (brown) is the normal of S and $\bar{\mathbf{n}}_{\mathbf{p}}$ (green) is the normal of B corresponding to \mathbf{p} .

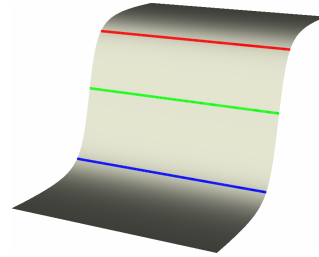


Figure 3. A 3D smooth step model. The green line is a relief edge, the red line is the corresponding ridge, and the blue line is the corresponding valley.

2.2. The prominent direction on the features

The prominent direction on the step edge is defined as the direction perpendicular to the ridge, valley, and relief edge. In practice, surfaces are not ideal step edges and thus we need to define the prominent field more carefully.

Let \mathbf{p} be a point on the surface, $\mathbf{g}_{\mathbf{p}}$ be the direction perpendicular to the relief edge, and $\mathbf{t}_{\mathbf{p}}$ be the first principal direction. On the step edge model, $\mathbf{g}_{\mathbf{p}}$ is meaningful only on the relief edge and $\mathbf{t}_{\mathbf{p}}$ is well-defined everywhere else, since the relief edge points are umbilical points. Therefore, to define the prominent direction $\mathbf{r}_{\mathbf{p}}$, we take a weighted combination of both directions, where the weight $\alpha_{\mathbf{p}}$ is 1 near relief edges and 0 at ridge/valley points.

Definition 2.1 The prominent direction is defined as

$$\mathbf{r}_{\mathbf{p}} = \alpha_{\mathbf{p}}\mathbf{g}_{\mathbf{p}} + (1 - \alpha_{\mathbf{p}})\mathbf{t}_{\mathbf{p}},$$

where $\alpha_{\mathbf{p}} \in [0, 1]$ is a scalar weight that determines the relative distance of \mathbf{p} from the relief edge.

Let κ_1 and κ_2 be the principal curvatures, k their ratio, and l the median length of mesh edges. Empirically, we observed that good results are obtained when

$$\alpha_{\mathbf{p}} = \begin{cases} 0 & |k| > 4 \text{ or } \max(|\kappa_1|, |\kappa_2|) < 3/l \\ 1 & |k| < 2 \\ \frac{4-|k|}{2} & \text{otherwise.} \end{cases} \quad (2)$$

2.3. The prominent direction on the whole surface

In the previous section we defined the prominent field on the features. To extend the definition to the whole surface, we search for the smoothest direction field that satisfies the values of the prominent field on the features.

Utilizing the Laplacian as the smoothness measure, we define the prominent field as the solution of the Poisson equation. The values of the prominent field on the features serve as boundary conditions for the equation.

Formally, we want to compute the prominent field $\mathbf{s}_{\mathbf{p}} = [s_{\mathbf{p}}^u, s_{\mathbf{p}}^v]$, such that the Laplacian $[\Delta s_{\mathbf{p}}^u, \Delta s_{\mathbf{p}}^v]$ of the field components is equal to zero and $\mathbf{s}_{\mathbf{p}} = \mathbf{r}_{\mathbf{p}}$ on the features. Let $\beta_{\mathbf{p}} \in [0, 1]$ be our confidence that \mathbf{p} is a feature point (explained below). Hence, at each point \mathbf{p} , the following should hold:

$$\begin{aligned} \beta_{\mathbf{p}} \mathbf{s}_{\mathbf{p}} &= \beta_{\mathbf{p}} \mathbf{r}_{\mathbf{p}}, \\ (1 - \beta_{\mathbf{p}}) \Delta s_{\mathbf{p}}^u &= 0, \\ (1 - \beta_{\mathbf{p}}) \Delta s_{\mathbf{p}}^v &= 0. \end{aligned} \quad (3)$$

Thus, on the features ($\beta_{\mathbf{p}} \approx 1$), the first equation enforces the boundary conditions and elsewhere, the two other equations enforce the smoothness of the solution.

We approximate the confidence value $\beta_{\mathbf{p}}$ such that it is close to one when the point is near an edge and zero otherwise. Recall that the points on the edge are characterized either by a high ratio between the principal curvatures (near ridges and valleys) or by a small difference between the surface S and its approximated step edge ϵ_r [12, Equation 7]. Specifically,

$$\beta_{\mathbf{p}} = \begin{cases} 1 & (|k| > 2 \text{ and } \max(|\kappa_1|, |\kappa_2|) > 3/l) \text{ or} \\ & \epsilon_r > 2/l \\ 0 & \text{otherwise,} \end{cases} \quad (4)$$

where l is the median length of the mesh edges.

To compute the prominent field $\mathbf{s}_{\mathbf{p}}$ we need to solve Equation 3. We do it by first deriving a linear approximation of the Laplacian $[\Delta s_{\mathbf{p}}^u, \Delta s_{\mathbf{p}}^v]$ of the components of the prominent field and then solving the set of linear equations in $\mathbf{s}_{\mathbf{p}}$.

To compute the Laplacian of a scalar function f on a surface, we follow [13]:

$$\begin{aligned} \Delta f(\mathbf{p}) &= \frac{1}{2A} \sum_{j \in N(\mathbf{p})} (\cot(\gamma_j) + \cot(\delta_j))(f(\mathbf{p}) - f(\mathbf{p}_j)), \\ &\equiv \frac{1}{2A} \sum_{j \in N(\mathbf{p})} w_j (f(\mathbf{p}) - f(\mathbf{p}_j)), \end{aligned} \quad (5)$$

where $N(\mathbf{p})$ is the set of the neighbors of point \mathbf{p} , A is the area of the Voronoi cell of \mathbf{p} , and γ_j and δ_j are the angles opposite the edge $[\mathbf{p}, \mathbf{p}_j]$ of the triangles sharing this edge.

$[\Delta s_{\mathbf{p}}^u, \Delta s_{\mathbf{p}}^v]$ cannot be computed directly using Equation 5, since the components $[s_{\mathbf{p}}^u, s_{\mathbf{p}}^v]$ of the prominent field are defined in the local tangent plane, which differs from point to point. To address this problem, we calculate the transformation between the local coordinate systems of the neighboring points and utilize it in the computation of the Laplacian.

This transformation is computed as follows. First, the tangent plane of point \mathbf{p}_j is rotated by aligning the normals of \mathbf{p} and \mathbf{p}_j . Next, the coordinate systems are aligned in the tangent plane, by applying a 2D rotation by θ : $R = [(\cos \theta, \sin \theta)^T, (-\sin \theta, \cos \theta)^T]$ (Figure 4). Finally, the Laplacian of the prominent field can be written as:

$$\begin{aligned} \Delta s_{\mathbf{p}}^u &= \frac{1}{2A} \sum_{j \in N(\mathbf{p})} w_j (s_{\mathbf{p}_j}^u - \cos \theta s_{\mathbf{p}}^u - \sin \theta s_{\mathbf{p}}^v), \\ \Delta s_{\mathbf{p}}^v &= \frac{1}{2A} \sum_{j \in N(\mathbf{p})} w_j (s_{\mathbf{p}_j}^v + \sin \theta s_{\mathbf{p}}^u - \cos \theta s_{\mathbf{p}}^v). \end{aligned} \quad (6)$$

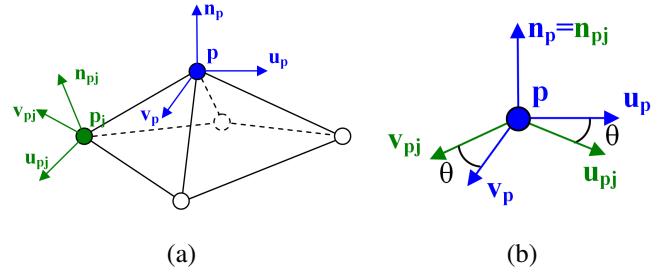


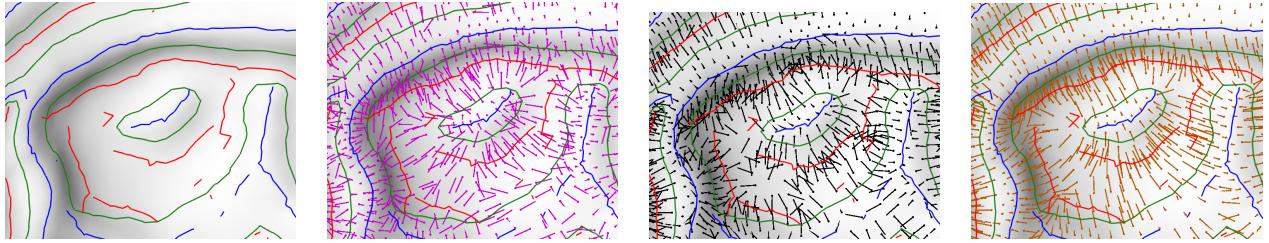
Figure 4. Alignment of the local coordinate systems. (a) First, we rotate the coordinate system of \mathbf{p}_j so that the tangent plane of \mathbf{p}_j coincides with the tangent plane of \mathbf{p} . The rotation is performed around the cross product of $\mathbf{n}_{\mathbf{p}}$ and $\mathbf{n}_{\mathbf{p}_j}$. (b) Then, the coordinate systems of \mathbf{p}_j and \mathbf{p} are registered by rotating the rotated tangent plane of \mathbf{p}_j by θ .

Using Equations 6 and 4, we now solve the linear system of Equation 3, yielding the prominent field. Finally, since the prominent field is a direction field, it is normalized. Note that after normalization, the Laplacian is not guaranteed to remain small. In practice, however, the change is negligible.

Figure 5 illustrates the construction of the prominent field on part of the object in Figure 10. It can be seen that the principal directions are meaningful near the ridges and valleys, but not between them. Moreover, the relief directions are meaningful between the ridges and valleys, but not on them. Our prominent field is meaningful everywhere.

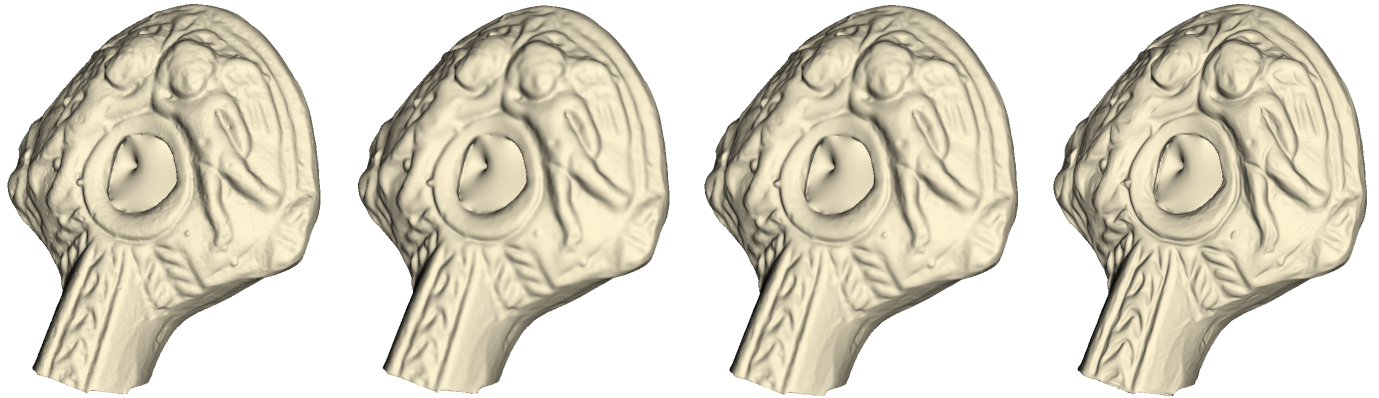
3. Surface enhancement and smoothing

Archaeological objects are often unsuitable for further processing and visual analysis, either due to erosion that they underwent during the ages or due to scanning noise.



(a) Feature curves (b) First principal direction (c) Relief direction (d) Prominent field

Figure 5. Construction of the prominent field. The prominent field (d) is a smooth combination of the first principal direction (b) and the relief direction (c). In contrast to its components, it is well-defined and smooth everywhere.



(a) The given object (b) Standard bilateral filtering (c) Our bilateral filtering (d) Our final result

Figure 6. Enhancement of a late Hellenistic oil lamp from the first century BCE

This section describes how to enhance and smooth these objects, to enable effective processing and analysis.

One way to address these problems is by using adaptive filtering algorithms, which smooth (or denoise) the surface, while keeping the features intact or enhancing them. Existing approaches for adaptive filtering on meshes operate either on the mesh vertices [5, 8, 22], the mesh normals [2, 17], or the curvatures [7]. The techniques differ in the energy functional they attempt to minimize.

While these approaches perform well preserving and enhancing ridges and valleys, they are not designed for relief objects. In particular, there are a couple of cases in which they may produce inferior results. The first case occurs when no distinct ridges or valleys can be detected on the surface. These approaches will simply smooth the objects, diminishing the 3D features, as seen in Figure 6(b). The second case occurs when there exist distinct valleys and ridges, but the slope of their step edge is shallow, as illustrated in Figure 7. In this case, these approaches aim at enhancing each of these features separately, but do not enhance the step edge model between them. Our goal is to preserve and enhance this step edge by steepening the slope of the step edge.

We propose a novel approach that solves these problems.



Figure 7. The cyan curve is the local image defined on the black base. Since this surface has sharp ridges and valleys, it will not be enhanced by standard adaptive filtering. The desired result, illustrated in orange, enhances the 3D feature.

It consists of two steps – bilateral filtering and inverse curvature flow – each makes use of our prominent field to guide the smoothing and enhancement directions. Though we describe a specific bilateral filtering, our prominent field can be combined with many other adaptive filtering techniques.

Bilateral filtering: A bilateral filter sets the position of a vertex to a weighted average of its neighbors. The weights depend both on the distance between the points and on their similarity. We propose to base the similarity component on the distance between the points along the prominent direction.

Let \mathbf{p} be a point on the surface, $N(\mathbf{p})$ be the set of its neighbors, $d_j = \|\mathbf{p} - \mathbf{p}_j\|$ be the Euclidean distance between \mathbf{p} and \mathbf{p}_j , and $\mathbf{n}_{\mathbf{p}}$ be the normal at \mathbf{p} . In [8] it is proposed to define the similarity as the distance between \mathbf{p}_j

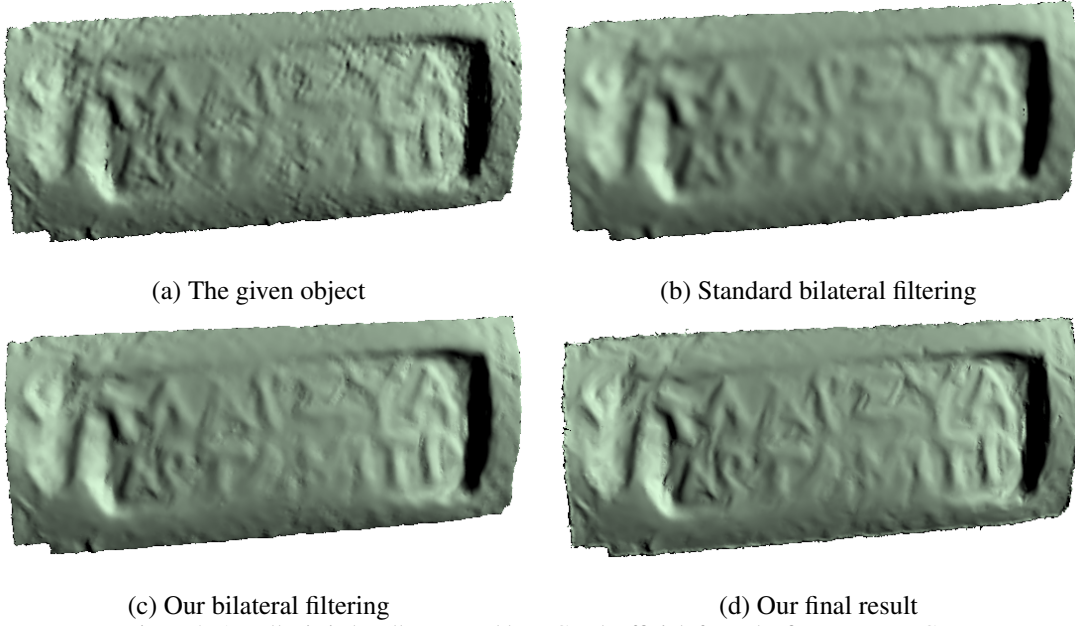


Figure 8. A Hellenistic handle stamped by a Greek official, from the first century BCE

and \mathbf{p} 's tangent plane: $h_j = |\langle \mathbf{n}_{\mathbf{p}}, \mathbf{p} - \mathbf{p}_j \rangle|$, so that smoothing is performed when \mathbf{p}_j is close to the tangent plane of \mathbf{p} . We propose to add to this definition a term that depends on r_j , the projection of $\mathbf{p} - \mathbf{p}_j$ along the prominent direction. Thus, smoothing will not be performed in the prominent direction. This is done by multiplying the weights suggested in [8] by the term $e^{-r_j^2/2\sigma_p^2}$.

Hence, our similarity-based change of \mathbf{p} in its normal direction is

$$\delta_{\mathbf{p}} = C \sum_{j \in N(\mathbf{p})} e^{-d_j^2/2\sigma_c^2} \cdot e^{-h_j^2/2\sigma_s^2} \cdot e^{-r_j^2/2\sigma_p^2} \cdot h_j, \quad (7)$$

yielding a new position for \mathbf{p} :

$$\mathbf{p}' = \mathbf{p} + \delta_{\mathbf{p}} \mathbf{n}_{\mathbf{p}}, \quad (8)$$

where, C is the normalization coefficient. In the implementation, $\sigma_s = 0.5\sigma_c$, $\sigma_p = 0.4\sigma_c$, and σ_c is a user-supplied parameter that determines the amount of smoothing. It is common to slightly smooth the object prior to computing the distances.

Figures 6(c) & 8(c) show the results obtained by applying our bilateral filtering to scans of real archaeological artifacts. In comparison to [8] (Figures 6(b) & 8(b)) it can be seen that the features are more pronounced.

Inverse-curvature flow: The inverse-curvature flow is a high frequency filter [1, 18, 19], which updates the position of a vertex so as to increase the absolute value of its curvature. It can be based on the mean, maximum, minimum, or any other type of curvature.

While the inverse-curvature flow manages to enhance features, it suffers from two drawbacks. First, it is an iterative process that does not have a well-defined stopping criterion. Second, it often creates spurious features on the surface, in addition to the enhanced features. This is so since in near-flat regions, points with locally higher-curvature values are enhanced.

We propose a new inverse-curvature flow, which is based on two modifications to the standard flow. First, the curvature is computed in the prominent direction, enhancing only the real features. Second, a new stopping criterion is suggested, which is based on the intuition in which a feature point should not exceed the maximum of the feature with respect to the base. Figure 9 illustrates the problem. The exaggerated edge (red) exceeds the original height of the feature (green). It is also possible to let the user decide interactively when to stop the process.

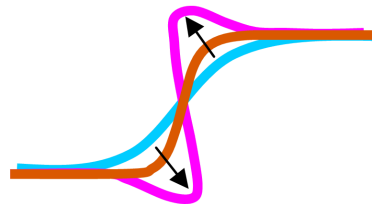


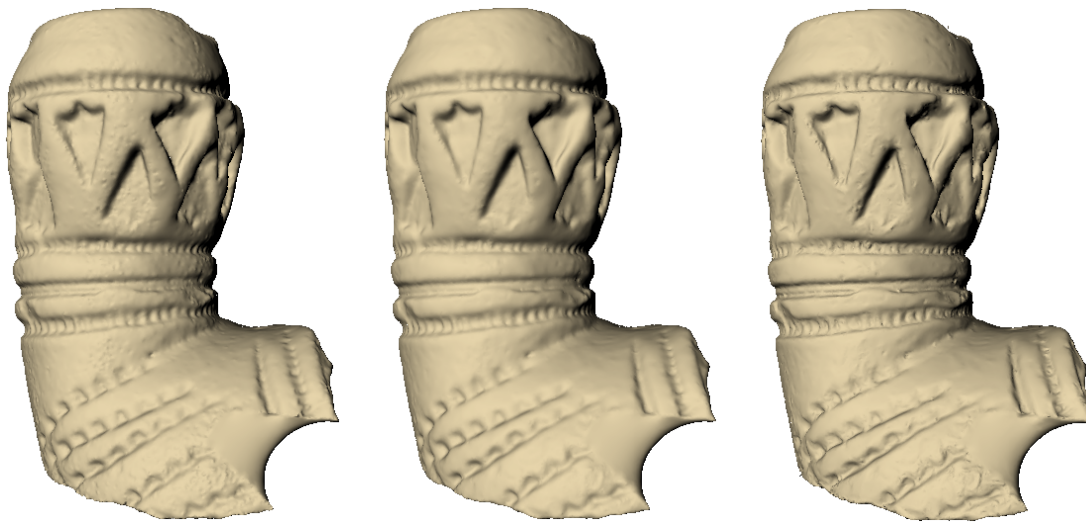
Figure 9. Inverse-curvature flow. The initial surface in cyan; the standard inverse-curvature flow in magenta, and our inverse-curvature flow in orange.

To do this, at each point the normal to the base surface is estimated [12]. Since the height is now locally defined with respect to the base, the local maximum (minimum) can be



(a) The given object (b) After our bilateral filtering (d) Our final result

Figure 10. A late Hellenistic oil lamp from the first century BCE



(a) The given object (b) After our bilateral filtering (d) Our final result

Figure 11. Ottoman pipe

tested. Hence, the stopping criterion can be enforced.

Results: Figures 6,8,10-11 illustrate some of our results. It can be seen that the inverse-curvature flow indeed enhances the features obtained after applying bilateral filtering, which removed the noise from the original surface.

4. Prominent coloring

Traditionally, archaeological artifacts are drawn by hand and printed in the reports of archaeological excavations, as illustrated in Figure 12. The artists utilize artificial coloring in order to enhance the three-dimensional features. Several kinds of computerized artificial coloring (shading) methods have been proposed in the literature [4, 9, 10, 15, 20], in which the object is colored according to its geometric properties. For instance, it is proposed in [10] to color the shape according to its mean curvature.

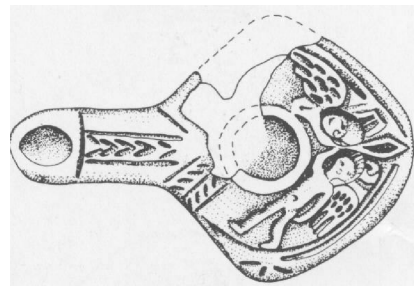
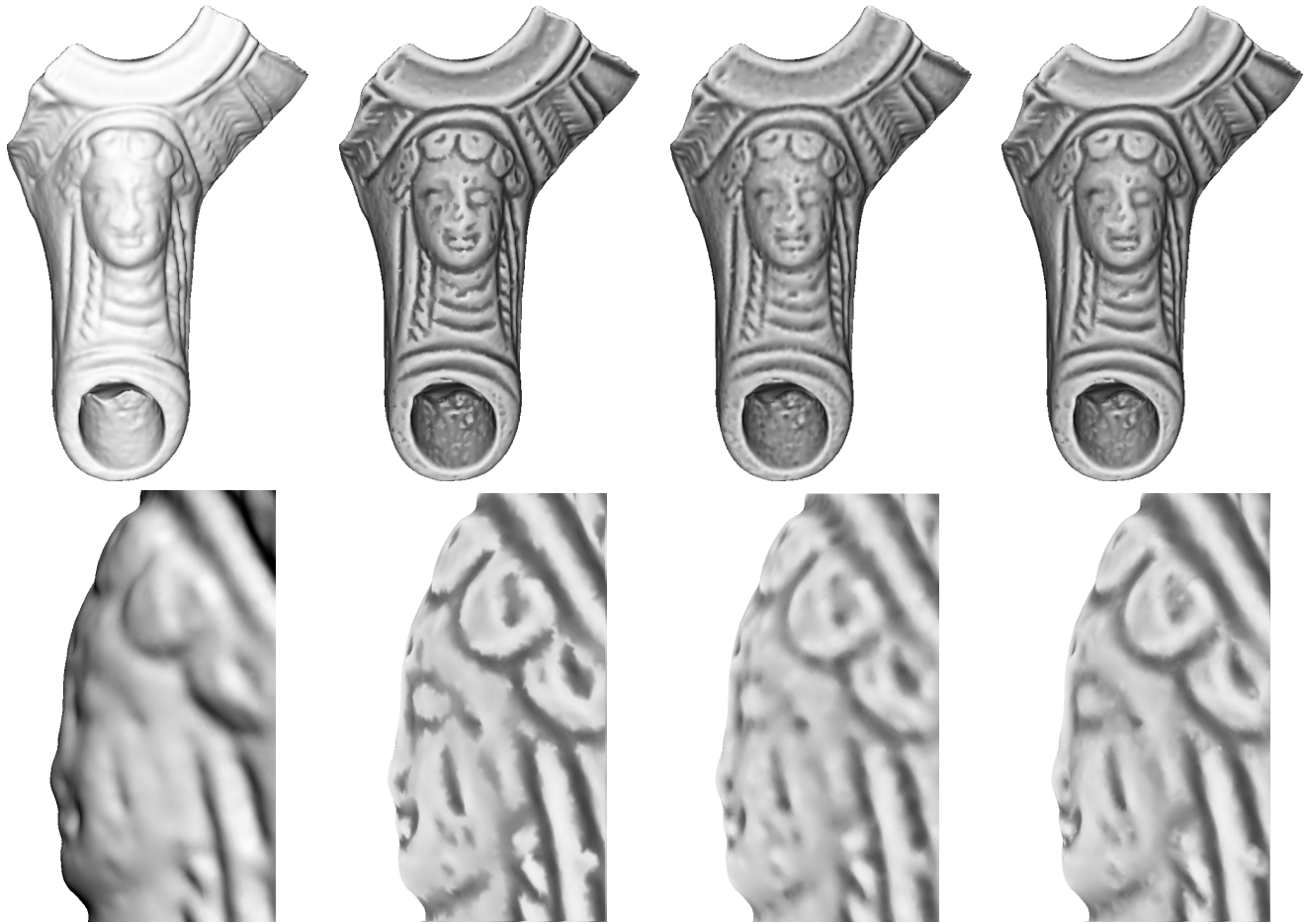


Figure 12. Manual illustration of an archaeological artifact [16]

We propose a new method for artificial coloring, termed *prominent coloring*. The color of a vertex is set according to its curvature in the prominent direction. The lower the curvature, the darker its color. Formally, given a vertex with



(a) The object (b) Max-curvature shading (c) Mean-curvature shading (d) Prominent coloring

Figure 13. Comparison of various coloring methods. Top: complete artifact; bottom: partial profile. Note that the maximal-curvature shading is noisy; the mean-curvature shading is blurred; our shading is crisper and less noisy. This is visible, for instance, on the eye, crown, and hair.

curvature prominent κ_p , its color is defined as

$$\text{color} = \arctan(\lambda\kappa_p), \quad (9)$$

where λ is a parameter.

Figures 13-14 show that indeed the prominent coloring emphasizes the transition between areas of positive and negative prominent curvature, i.e., the transition between ridges and valleys. It can be seen that the maximal-curvature shading is noisy and the mean-curvature shading is blurred, while the prominent coloring is crisper.

5. Conclusions

This paper addressed the problem of automatic processing of scanned artifacts. The processing is based on a definition of a new field – the prominent field. The prominent field is computed in interactive time (a couple of seconds for 100,000 vertices). We demonstrated how to employ the

prominent field for surface smoothing and enhancement and for artificial surface coloring, which emphasizes the object features. In both cases, the methods were applied to archaeological artifacts, which are typically noisy and suffered erosion over time.

In the future, we intend to apply our prominent field to other applications, such as shape matching and reconstruction.

Acknowledgements

This research was supported in part by the Israel Science Foundation (ISF) 628/08, Olendorff foundation and the joint Technion University of Haifa research foundation. We thank Dr. A. Gilboa and Zinman Institute of Archaeology for supplying us the models and for fruitful discussions on the topic.



(b) Maximal-curvature shading

(c) Mean-curvature shading

(d) Prominent coloring

Figure 14. Comparison of various shading methods

References

- [1] C. Bajaj and G. Xu. Anisotropic diffusion of surfaces and functions on surfaces. *ACM Transactions on Graphics (TOG)*, 22(1):4–32, 2003.
- [2] Y. Belyaev and H. Seidel. Mesh smoothing by adaptive and anisotropic Gaussian filter applied to mesh normals. *Vision, Modeling, and Visualization*, pages 203–210, 2002.
- [3] B. Brown, C. Toler-Franklin, D. Nehab, M. Burns, D. Dobkin, A. Vlachopoulos, C. Doumas, S. Rusinkiewicz, and T. Weyrich. A system for high-volume acquisition and matching of fresco fragments: reassembling Theran wall paintings. *ACM Trans. Graph.*, 3(27), 2008.
- [4] J. Cohen, D. Duncan, D. Snyder, J. Cooper, J. Kumar, S. Hahn, D. Chen, B. Purnomo, and J. Graettinger. iclay: Digitizing cuneiform. *Symposium on Virtual Reality, Archaeology and Cultural Heritage*, pages 135–143, 2004.
- [5] M. Desbrun, M. Meyer, P. Schroder, and A. Barr. Implicit fairing of irregular meshes using diffusion and curvature flow. *ACM Transactions on Graphics (TOG)*, 17(3):317–324, 1999.
- [6] M. P. Do Carmo. *Differential geometry of curves and surfaces*. Prentice-Hall, 1976.
- [7] M. Eigensatz, R. Sumner, and M. Pauly. Curvature-domain shape processing. *Comp. Graph. Forum*, 27(2):241–250, 2008.
- [8] S. Fleishman, I. Drori, and D. Cohen-Or. Bilateral mesh denoising. *ACM Transactions on Graphics (TOG)*, 22(3):950–953, 2003.
- [9] B. Gooch, P. J. Sloan, A. Gooch, P. Shirley, and R. F. Riesenfeld. Interactive technical illustration. *Symp. on Inter. 3D Graph.*, pages 31–38, 1999.
- [10] G. Kindlmann, R. Whitaker, T. Tasdizen, and T. Moller. Curvature-based transfer functions for direct volume rendering: Methods and applications. *IEEE Trans. on Vis. and Comp. Graph.*, pages 67–76, 2003.
- [11] D. Koller, J. Trimble, T. Najbjerg, N. Gelfand, and M. Levoy. Fragments of the city: Stanford’s digital forma urbis romae project. *J. of Roman Arch.*, pages 237–252, 2006.
- [12] M. Kolomenkin, I. Shimshoni, and A. Tal. On edge detection on surfaces. *CVPR*, pages 2767–2774, 2009.
- [13] M. Meyer, M. Desbrun, P. Schroder, and A. H. Barr. Discrete differential-geometry operators for triangulated 2-manifolds. *VisMath*, B(207):187–217, June 2002.
- [14] H. Rushmeier. Eternal Egypt: experiences and research directions. *Recording, Modeling and Visualization of Cultural Heritage*, pages 22–27, 2006.
- [15] S. Rusinkiewicz, M. Burns, and D. DeCarlo. Exaggerated shading for depicting shape and detail. *NPAR*, pages 1199–1205, 2006.
- [16] E. Stern. *Excavations at Dor*. Jerusalem: Institute of Archaeology of the Hebrew University, 1995.
- [17] X. Sun, P. Rosin, R. Martin, and F. Langbein. Fast and effective feature-preserving mesh denoising. *IEEE Trans. on Vis. and Comp. Graph.*, 13(5):925–938, 2007.
- [18] T. Tasdizen, R. Whitaker, P. Burchard, and S. Osher. Geometric surface smoothing via anisotropic diffusion of normals. *IEEE Trans. on Vis. and Comp. Graph.*, pages 125–132, 2002.
- [19] G. Taubin. A signal processing approach to fair surface design. *Comp. grap. and interact. techn.*, pages 351–358, 1995.
- [20] C. Toler-Franklin, A. Finkelstein, and S. Rusinkiewicz. Illustration of complex real-world objects using images with normals. *NPAR*, pages 111–119, 2007.
- [21] A. Vrabel, O. Bellon, and L. Silva. A 3D Reconstruction Pipeline for Digital Preservation. *CVPR*, pages 2687–2694, 2009.
- [22] S. Yoshizawa, A. Belyaev, and H. Seidel. Smoothing by example: Mesh denoising by averaging with similarity-based weights. *IEEE Int. Conf. on Shape Model. and App.*, pages 9–19, 2006.